

Synthesis of Novel Ionic Polymers Containing Arsonic Acid Group

J. GARCÍA-SERRANO,^{1,2} A. M. HERRERA,² F. PÉREZ-MORENO,² M. A. VALDEZ,³ U. PAL¹

¹Instituto de Física, Universidad Autónoma de Puebla, Apdo. Postal J-48, Puebla, Pue. 72570, Mexico

²Centro de Investigaciones en Materiales y Metalurgia, Universidad Autónoma del Estado de Hidalgo, Carretera Pachuca Tulancingo Km 4.5, Pachuca, Hidalgo, Mexico

³Instituto de Física, Universidad de Sonora, Rosales y Transversal s/n. Hermosillo, Sonora. C.P. 83000, Mexico

Received 21 January 2006; revised 3 March 2006; accepted 4 March 2006

DOI: 10.1002/polb.20807

Published online in Wiley InterScience (www.interscience.wiley.com).

ABSTRACT: Synthesis of *ortho*- and *para*-acryloylaminophenylarsonic acids (*o*-AAPHA and *p*-AAPHA) monomers and their homopolymers, useful as ion-exchange materials, are reported. Both the monomers and homopolymers are synthesized with >90% yield. The structures of the new compounds are determined by NMR and FTIR spectroscopy. Molecular weights of the polymers are determined from light scattering measurements and found to be $M_w = 38,759$ g/mol for *o*-AAPHA polymer and $M_w = 31,347$ g/mol for *p*-AAPHA polymer. Good thermal stability of the new compounds derived from their intra- or intermolecular hydrogen bondings suggests their applications as proton-exchange membrane at high temperatures. ©2006 Wiley Periodicals, Inc. *J Polym Sci Part B: Polym Phys* 44: 1627–1634, 2006

Keywords: FTIR; ion-exchange polymers; light scattering; metallorganic compounds; NMR; synthesis

INTRODUCTION

In recent years, extensive efforts have been devoted to the development of new ionomers and polyelectrolytes for their applications in fuel cells,¹ water splitting,² electro-organic synthesis,³ catalysis,⁴ and nanoparticle synthesis.⁵ Ionomers are defined as polymers with a relatively small content of ionic groups.⁶ One of the most important characteristics of the ionomers is the nature of their low content monomers with specific ionic group, which are responsible for proton exchange in the aforementioned processes.

The most common ionic groups used in the preparation of ionomer membranes are the carboxylic, sulfonic, and phosphonic acid groups, although recently the use of different heteropolyacids like silicotungstic acid,⁷ phosphotungstic acid, phosphomolybdic acid, or phosphotitanic acid⁸ has been reported. All the ionomers have been studied for their potential applications as proton-exchange membrane (PEM) in fuel cells. Among the PEMs for polymer electrolyte fuel cell applications, the perfluorsulfonic acid polymer Nafion[®] is the one which has been studied most extensively. However, the high cost, complicated manufacturing process, high methanol permeability, and poor performance at temperatures above 80 °C due to loss of water are its main drawbacks, which lead to the development of new PEMs to replace it.

Though the successful use of carboxylic, sulfonic, and phosphonic acid groups to prepare PEMs with efficient ion-exchange characteris-

This article contains supplementary material available via the Internet at <http://www.interscience.wiley.com/jpages/0887-6266/suppmat>

Correspondence to: U. Pal (E-mail: upal@sirio.ifuap.buap.mx)

Journal of Polymer Science: Part B: Polymer Physics, Vol. 44, 1627–1634 (2006)
©2006 Wiley Periodicals, Inc.

tics⁹ has been reported, there is no report on the synthesis of ionomers or polyelectrolytes with arsonic acid side group. —AsO(OH)₂ group is a proton exchanger very similar to phosphonic acid that has been largely used in analytical separation of different metals such as Al, Be, In, Th, and Zr¹⁰ as well as for concentrating and separation of trace metal ions from hard- and sea-water.¹¹ Arsonic acid compounds manifest enhanced selectivity to metal cations in the order of Mg²⁺ < Ca²⁺ < Mn²⁺ < Co²⁺ < Ni²⁺ < Zn²⁺ < Cu²⁺.¹² Owing to the ion-exchange capacity and selectivity of the —AsO(OH)₂ functional group, polymers containing this group might have potentials for use as PEMs in fuel cells. Though its lower acidity in comparison with the sulfonic acid group may result in slower ion-exchange process at high pH values, its capacity to interexchange two protons might be advantageous in PEM applications.

In the present work, we report the synthesis, characterization, and polymerization of two new metallorganic monomers containing arsonic acid group (AsO(OH)₂) attached covalently to the phenyl ring of the molecule: the *o*-acryloylaminophenylarsonic acid (*o*-AAPHA) and *p*-acryloylaminophenylarsonic acid (*p*-AAPHA). In the first, the arsonic acid group is localized at the ortho-position of the phenyl group, whereas in the second, the arsonic acid group is placed at the para-position and relatively distant from the double bond site of the alkene group. The polymerization of *o*- and *p*-AAPHA was carried out via free radicals, using 2,2'-azoisobutyronitrile (AIBN) as a free radical initiator. Formation and molecular structures of the synthesized monomers and polymers were confirmed from their ¹H NMR, ¹³C NMR, and infrared (IR) spectra as well as from their elemental analysis. Molecular weights of the polymers were determined by light scattering measurements. Thermal stabilities of the new compounds were studied by thermogravimetric analysis (TGA).

EXPERIMENTAL

Materials

o-Arsanilic acid was purchased from Sigma-Aldrich. *p*-Arsanilic acid and acryloyl chloride were purchased from Fluka Co. Acryloyl chloride was purified by distillation. Initiator AIBN was recrystallized using methanol. All solvents were used as delivered.

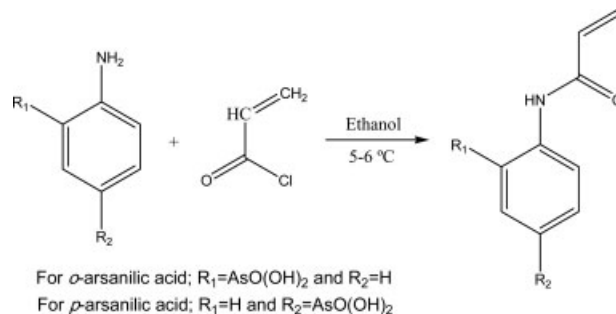


Figure 1. Condensation reaction of the *o*-arsanilic acid or *p*-arsanilic acid with acryloyl chloride.

Synthesis of *o*-AAPHA and *p*-AAPHA

The monomers were obtained by condensation of acryloyl chloride with the corresponding arsanilic acid (Fig. 1). A 100 mL three-necked flask equipped with a mechanical stirring device was charged with 10 g (46.10 mmol) of *o*-arsanilic acid (or *p*-arsanilic acid), and then 40 mL of ethanol was added under stirring. After the complete dissolution of the *o*- or *p*-arsanilic acid, 3.72 mL (46.15 mmol) of pyridine was added, and the mixture was cooled to 5–6 °C in an ice bath, followed by a drop wise addition of 3.75 mL (46.15 mmol) of freshly distilled acryloyl chloride. The temperature of the exothermic reaction was maintained at 5–6 °C under stirring for 20 h. The resultant mixture was carefully poured into 100 mL of acetone, obtaining a white precipitate with a 98% yield. For purification, the crude compounds were dissolved in ethanol–water (80:20) mixture and recrystallized. The solid was filtered off, washed with water, and dried at 80 °C in vacuum for 12 h.

Synthesis of Poly(*o*-AAPHA) and Poly(*p*-AAPHA)

The monomers *o*-AAPHA and *p*-AAPHA acids were polymerized in DMF solution, using AIBN as a free radical initiator. 1.694 g (6.25 mmol) of monomer and 4.2 mg (0.026 mmol) of initiator were completely dissolved in 25 mL of DMF in a glass test tube and bubbled with argon gas for 20 min. The test tube was then sealed under argon and placed in a constant temperature (70 °C) water bath for 48 h. After this period, the reaction mixture was cooled to room temperature, and the polymers were isolated by precipitation of the viscous products in acetone (10 times the volume of the reaction mixture), and with subsequent drying at 80 °C in vacuum for



Figure 2. Photographs of the powdered *o*-AAPHA (left) and *p*-AAPHA (right) samples. [Color figure can be viewed in the online issue, which is available at www.interscience.wiley.com.]

12 h. The polymers of *o*-AAPHA and *p*-AAPHA were obtained with a (1.517 g) 89 and (1.643 g) 97% yield, respectively. Both the polymers were obtained in a powder form. While the *p*-AAPHA polymer was white in color, the *o*-AAPHA polymer was of light yellow-brown (Fig. 2).

Characterizations

^1H NMR and ^{13}C NMR spectra of the samples were recorded on Varian Mercury 400 (400 MHz/100 MHz) or Varian Mercury 300 (300 MHz/75 MHz) NMR spectrometer, using deuterated DMSO and D_2O as the solvents and TMS as the internal reference. IR spectra were recorded on a Perkin–Elmer Spectrum GX FTIR spectrophotometer, with a spectral resolution of 4 cm^{-1} . Elemental analysis (C, H, N) of the samples was carried out on a Perkin–Elmer C, H, N analyzer (model 2400). Thermogravimetric measurements of the monomers and polymers were carried out with a Mettler Toledo thermal gravimetric analyzer (model 851). The measurements were performed from room temperature to $550\text{ }^\circ\text{C}$, at a heating rate of $10\text{ }^\circ\text{C}/\text{min}$ under nitrogen atmosphere. Average molecular weights of the polymers were determined by static light scattering measurements using a ALV-5000 digital correlator system (Langen-GmbH, Germany)

Journal of Polymer Science: Part B: Polymer Physics
DOI 10.1002/polb

fitted with a temperature controller set at $25 \pm 0.1\text{ }^\circ\text{C}$. For light scattering measurements, samples of *o*- and *p*-AAPHA polymers were dissolved in DMF and water respectively, in three different concentrations: 21.6, 25, and 29 mg/mL for *o*- and *p*-AAPHA; 3.4, 5.2, and 7.0 mg/mL for *p*-AAPHA. A vertically polarized argon laser (30 mW, $\lambda_0 = 632\text{ nm}$) was used as excitation source. The intensity of the scattered light was measured at an angle of 90° . The reduced elastic scattering $I(q)/Kc$, with $K = 4\pi^2 n_0^2 (dn/dc)^2 (I^{90}/R^{90})/\lambda_0^4 N_A$, was measured, where n_0 is the refractive index of the standard (toluene, 1.339), c is the sample concentration in g/mL, $I(q)$ is the intensity scattered by the sample, and N_A is the Avogadro's number. I^{90} and R^{90} are the scattered intensity and the Rayleigh ratio for the standard at $\theta = 90^\circ$, respectively. The increment of refractive index of the polymer solutions (dn/dc) was measured with a refractometer (Mettler-Toledo, model RE4OD), resulting in 0.1386 L/mg for *o*-AAPHA and 0.1817 L/mg for *p*-AAPHA. The expression of the scattering angle q is given by: $q = (4\pi n/\lambda_0) \sin(\theta/2)$. A Zimm plot was constructed to extract the average molecular weight using the following equation¹³:

$$Kc/R^{90} = (1/M) + 2Ac \quad (1)$$

where M is the average molecular weight and A is the second virial coefficient. The average molecular weight was obtained from the Y-axis intercept of the Kc/R^{90} versus c plot at $c = 0$.

RESULTS AND DISCUSSION

Monomer Characterizations

The *o*-AAPHA was found to be soluble in polar solvents like ethanol, methanol, water, DMF, and DMSO at room temperature; whereas *p*-AAPHA was soluble in methanol, DMF, and DMSO, and partially soluble in ethanol and water. Both the monomers were insoluble in toluene, ether, chloroform, acetone, tetrahydrofuran, benzene, and hexane. Elemental analysis revealed 39.89% C, 3.73% H, and 4.22% N contents in the monomers; whereas, their exact formula values for the compound $\text{C}_9\text{H}_{10}\text{O}_4\text{NAs}$ would have been 39.87, 3.71, and 5.16%, respectively.

The ^1H NMR and ^{13}C NMR spectroscopic results of the synthesized monomers are summarized in Tables 1–3. The most important signals for both the compounds, which indicate their forma-

Table 1. Assignment of ^1H NMR Peak Positions of the *o*-AAPHA Acid Monomer

Chemical Shift δ (ppm)	Integration	Multiplicity	$J_{\text{H-H}}$ (Hz)	Assignment	Structure
11.96	1	s		H(NH)	
8.57	1	t	8.8	H ⁹	
7.70	1	d	7.34; 6.36	H ⁶	
7.62	1	t	7.32; 8.8	H ⁸	
7.27	1	t	7.32; 7.36	H ⁷	
6.31	1	m	8.32; 8.8	H ¹	
6.25	1	m	7.32; 9.8	H ¹	
5.80	1	t	9.8	H ²	

s, singlet; d, doublet; t, triplet; m, multiplet.

tion, were the multiplets assigned to the protons on the $\text{CH}_2=\text{C}$ at 6.31 and 6.25 ppm for *o*-AAPHA acid and at 6.45 and 6.30 ppm for *p*-AAPHA acid monomer, respectively. The ^1H NMR signal that appeared at 5.80 ppm, for both the monomers, was assigned to the proton of the CH, and the singlets at 11.96 and 10.52 ppm were assigned to the protons of the amide group of *o*-AAPHA and *p*-AAPHA respectively. The ^1H NMR data of the *o*-AAPHA acid revealed four signals at 8.57, 7.70, 7.62, and 7.27 ppm, arising from four different aromatic protons, whereas the *p*-AAPHA acid revealed signals at 7.88 and 7.73 ppm due to its two different types of aromatic protons. In the ^{13}C NMR spectra, the signal of the amide group carbon appeared at 164 ppm for both the monomers; while the signals corresponding to the vinylic carbons appeared at 129.13 and 132.48 ppm for *o*-AAPHA and at 128.58 and 132.04 ppm for *p*-AAPHA. Finally, the signals of the aromatic carbons were localized between 120 and 144 ppm for both the monomers.

Formation of the acid monomers is also evident from their IR spectra (Fig. 3), where the absorption bands due to primary amine group are absent. The

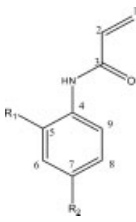
spectrum of the *o*-AAPHA acid revealed the bands due to the C=O stretching vibration mode (amide I band) at 1662 cm^{-1} , N—H bending (amide II band) at 1546 cm^{-1} , C—N stretching (amide III band) at 1279 cm^{-1} , all of secondary amide group; and C=C stretching at 1621 cm^{-1} of vinyl group. Also, there appeared intense bands in the range of $900\text{--}700\text{ cm}^{-1}$ due to As—O stretching. Further, the IR spectra of the monomer revealed absorption bands at 3120 (N—H stretch), 2213 (O—H stretch), and 1643 cm^{-1} (C=O stretch), confirming the presence of three different types of hydrogen bonds, as identified from its crystallographic data.¹⁴ Such observations are not unexpected, since our compounds have donor and acceptor groups, and hydrogen bond formation between them is favorable. The occurrence of N—H stretching band at frequencies lower than 3400 cm^{-1} indicates the participation of secondary amide N—H group in the hydrogen bond formation.¹⁵ We believe that this band arises from an intramolecular hydrogen bond involving the atoms N—H...O—As in a single monomer. Although the bands located at 2213 and 1643 cm^{-1} correspond to the intermolecular O—H...O—As¹⁶ and C=O...H—O hydrogen bonding, respectively.

Table 2. Assignment of ^1H NMR Peak Positions of the *p*-AAPHA Acid Monomer

Chemical Shift δ (ppm)	Integration	Multiplicity	$J_{\text{H-H}}$ (Hz)	Assignment	Structure
10.52	1	s		H(NH)	
7.88	2	d	5.6; 8.8	H ⁶	
7.73	2	d	5.8; 8.8	H ⁵	
6.45	1	m	7.32; 9.8	H ¹	
6.30	1	m		H ¹	
5.80	1	d	1.6; 1.2	H ²	

s, singlet; d, doublet; m, multiplet.

Table 3. Assignment of ^{13}C NMR Peak Position of the *o*-AAPHA and *p*-AAPHA Acid

	Chemical Shift δ (ppm)		Structure
	<i>o</i> -AAPHA	<i>p</i> -AAPHA	
C ¹	129.13	128.58	
C ²	132.48	132.04	
C ³	164.85	164.21	
C ⁴	141.32	143.51	
C ⁵	122.61	120.18	
C ⁶	132.12	131.67	
C ⁷	125.42	128.20	
C ⁸	135.11		
C ⁹	121.60		

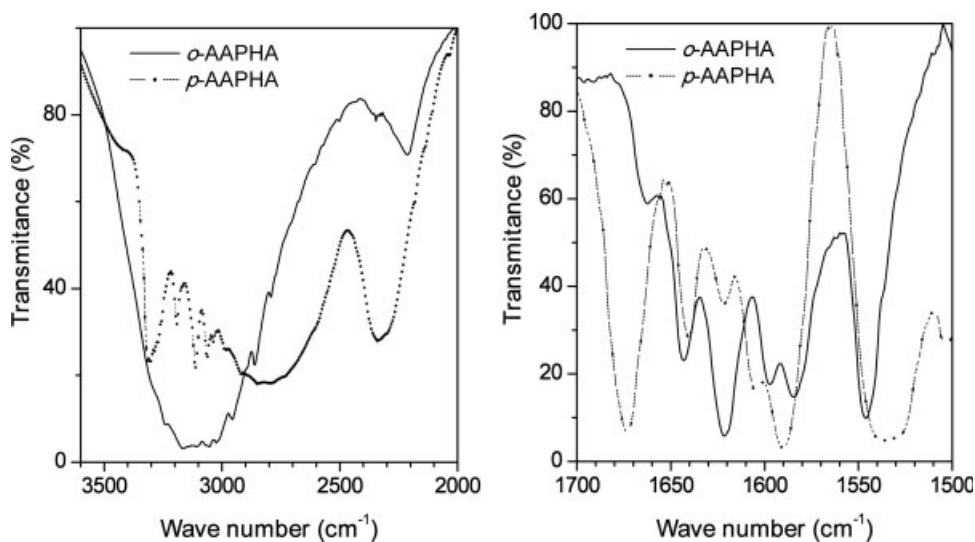
Structure determination by X-ray diffraction of the monomer revealed¹⁴ a 12.2° dihedral angle between the acrylamide group ($\text{CH}_2=\text{CHCONH}-$) and the carbon atom of the benzene ring. Such conformation allows the formation of an intramolecular hydrogen bond between the NH group of amide and the O atom of the arsonic group. Crystal structure of *o*-AAPHA is built up from classical centrosymmetric double hydrogen bonds involving O and OH of the arsonic acid, forming dimers connected in turn through a hydrogen bond between the OH group of arsonic acid (as donor) and the O atom of the amide functionality (as acceptor). The resulting network in the crystal is a 1-D chain.

The *p*-AAPHA acid IR spectrum, in addition to the bands due to As—O stretching modes,

exhibits the bands corresponding to the vibrational modes of C=O stretching (amide I band) at 1673 cm^{-1} , N—H bending (amide II band) at 1537 cm^{-1} , C—N stretching (amide III band) at 1295 cm^{-1} of secondary amide group, and C=C stretching at 1621 cm^{-1} of vinyl group, respectively. In this case, the N—H stretch region of IR spectrum revealed a band at 3310 cm^{-1} , with a shoulder at 3440 cm^{-1} , which indicates the existence of both hydrogen bonding and free secondary amide N—H groups¹⁷ in the sample. In *p*-AAPHA, as the $-\text{AsO}(\text{OH})_2$ group is placed at the para-position of the phenyl group, the intramolecular hydrogen bonding is impossible, and only the intermolecular N—H \cdots O—As hydrogen bonds can be formed. The bands observed at 2340 and 1641 cm^{-1} can be associated with the presence of intermolecular O—H \cdots O—As and C=O \cdots H—O hydrogen bonds in solid state.

Polymer Characterizations

The *p*-AAPHA polymer was soluble in highly polar solvents like DMF, water, and DMSO; whereas, the *o*-AAPHA polymer was soluble only in DMF and DMSO. Elemental analysis revealed 38.52, 4.52, and 5.93% of C, H, and N, respectively, for the *o*-AAPHA and 38.81, 4.81, and 5.63% of C, H, and N, respectively, for the *p*-AAPHA polymers. Our light scattering measurements offered $M_w = 38,759\text{ g/mol}$ for *o*-AAPHA and $M_w = 31,347\text{ g/mol}$ for *p*-AAPHA polymers, respectively.

**Figure 3.** IR spectra of *o*-AAPHA and *p*-AAPHA monomers in the spectral range of $3600\text{--}2000\text{ cm}^{-1}$ and $1700\text{--}1500\text{ cm}^{-1}$.

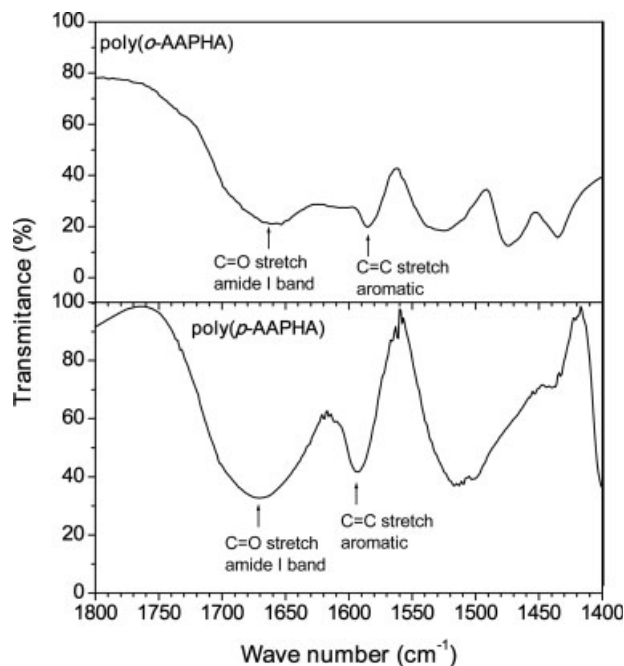


Figure 4. IR spectra of the polymers in the spectral range of 1800–1400 cm^{-1} .

Formation of the polymers was followed by ^1H NMR and IR spectroscopies. Principal evidence of polymer formation came from the disappearance of the protonic signals on the $\text{CH}_2=\text{C}$ of the monomers and the subsequent appearance of the methylenic proton signals in between 2.4 and 3.0 ppm for the polymers. Also, the signals corresponding to the aromatic protons were observed in the 6.5–8.0 ppm interval. Figure 4 shows the IR spectra of the *o*- and *p*-AAPHA polymers, where the absorption band due to $\text{C}=\text{C}$ stretching of vinyl group is absent, confirming the formation of the polymers. The peaks corresponding to the $\text{C}=\text{O}$ stretching vibrational modes of secondary amide group appeared at 1663 and 1672 cm^{-1} for *o*- and *p*-AAPHA polymers, respectively. The absence of the absorption band corresponding to the intermolecular $\text{C}=\text{O}\cdots\text{H}-\text{O}$ hydrogen bonding indicates that the hydrogen bond interactions are markedly reduced in the polymers.

Thermal Stability

The thermal stabilities of the new monomers and polymers are studied through thermogravimetric measurements (Fig. 5). The thermogravi-

metric curve of *o*-AAPHA [Fig. 5(a)] shows three distinct regions of weight loss with the increase of temperature. The first, a gradual weight loss of about 15.5% beginning at 120 $^\circ\text{C}$ and ending at 176 $^\circ\text{C}$, is associated to the residual water loss. In the second region, about 33% of the weight is lost between 280 and 330 $^\circ\text{C}$. This weight loss is probably due to the initial decomposition of organic components. Above 340 $^\circ\text{C}$, a complete decomposition of the organic components of *o*-AAPHA occurs. For the *p*-AAPHA, the thermogravimetric curve shows a 6.45% weight loss in between 185 and 218 $^\circ\text{C}$. The *p*-AAPHA shows excellent thermal stability up to 340 $^\circ\text{C}$ and then a drastic weight loss in between 360 and 450 $^\circ\text{C}$. These weight losses represent the residual water release and decomposition of organic components respectively.

Figure 5(b) shows the thermogravimetric curves for the polymers. While the *o*-AAPHA loses about 7.7% of weight in between 62 and 205 $^\circ\text{C}$, the *p*-AAPHA loses about 11% of weight in between 69 and 273 $^\circ\text{C}$. Such a gradual weight loss in the polymers can be attributed entirely to the loss of water from them. Above 330 $^\circ\text{C}$, the final decomposition of the polymers begins.

As shown in Figure 5, the *p*-AAPHA compounds are thermally more stable than the corresponding *o*-AAPHA compounds, since both the water loss and initial decomposition begin at higher temperatures for the former. These results suggest that the intermolecular hydrogen bonding in *p*-AAPHA compounds give a better thermal stability than do their ortho counterparts where the intramolecular hydrogen bonding is in vogue. The process of dehydration in polymers starts at higher temperatures than in the monomers and ends at significantly higher temperatures. While the weight loss curves for the monomers show clearly separated regions, indicating the involvement of distinct decomposition processes, absence of such distinct weight loss regions for the polymers indicate that the decomposition process in them is rather complicated.

CONCLUSIONS

In conclusion, new metal–organic compounds containing $\text{AsO}(\text{OH})_2$ group capable of cation exchange are synthesized. The *o*-AAPHA acid forms both intramolecular and intermolecular hydrogen bonds,

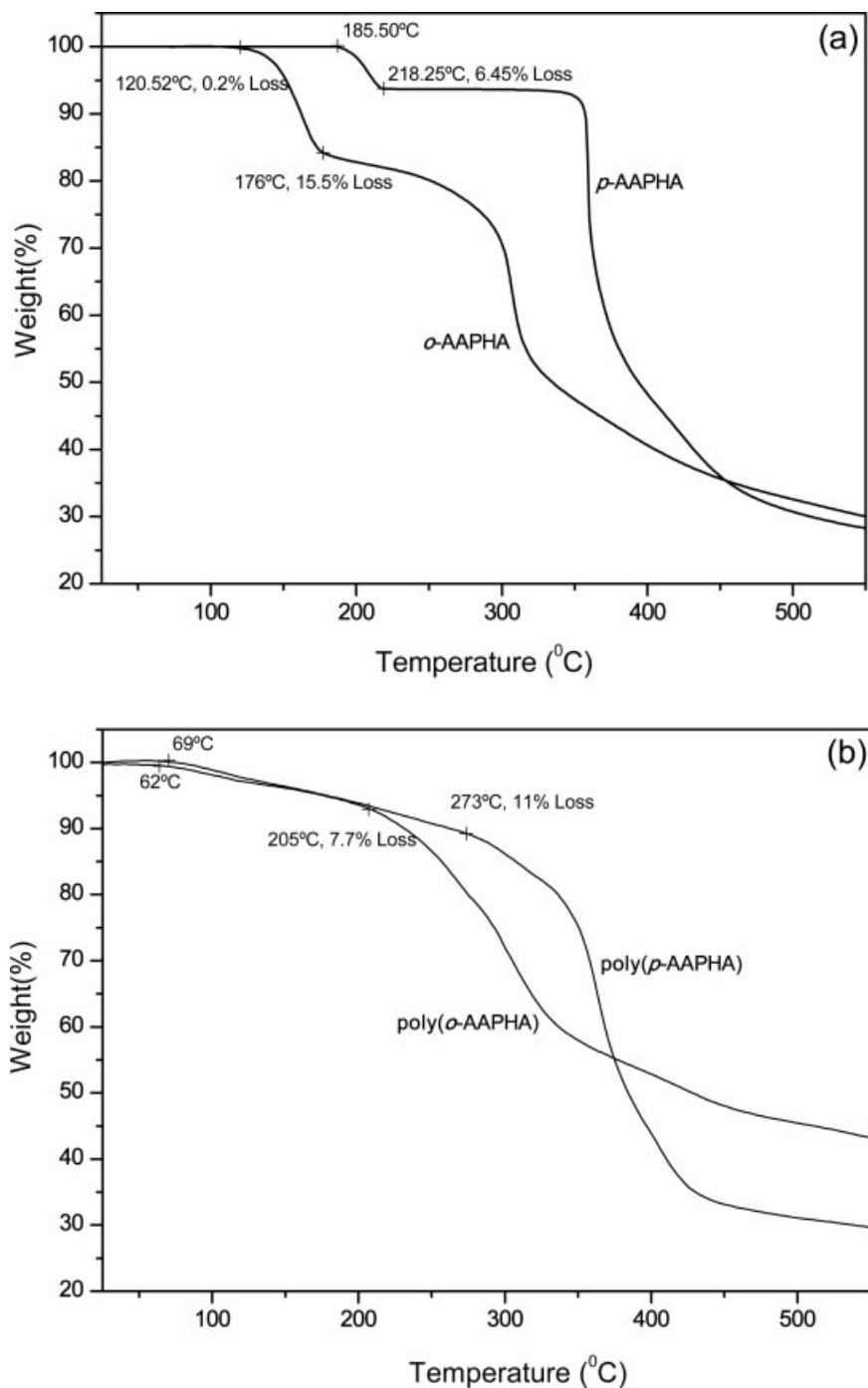


Figure 5. TGA curves of the (a) monomers and (b) polymers.

and the *p*-AAPHA acid forms only intermolecular hydrogen bonds. The hydrogen bond concentration in the compounds reduces drastically on polymerization. *o*-AAPHA, *p*-AAPHA, and their polymers are of good thermal stability. Owing to the ion-exchange capacity and good thermal stability of these new compounds they should be the promising can-

didates for the applications as thermally stable PEMs.

J. García-Serrano acknowledges to PROMEP, Mexico, for the graduate fellowship. The work was partially supported by VIEP-BUAP-CONACyT, Mexico, through Grant No. 11/I/EXC/05.

REFERENCES AND NOTES

1. (a) Kerres, J. A. *J Membr Sci* 2001, 185, 3; (b) Itoh, T.; Hamaguchi, Y.; Uno, T.; Kubo, M.; Aihara, Y.; Sonai, A. *Solid State Ionics* 2006, 177, 185.
2. Linkous, C. A.; Anderson, H. R.; Kopitzke, R. W.; Nelson, G. L. *Int J Hydrogen Energy* 1998, 23, 525.
3. Madden, T. H.; Stuve, E. M.; *J Electrochem Soc* 2003, 150, E571.
4. Bryant, D. E.; Kilner, A. *J Mol Catal A* 2003, 193, 83.
5. Hong, L.; Zhou, Y. J.; Chen, N. P.; Li, K. *J Colloid Interface Sci* 1999, 218, 233.
6. Eisenberg, A. *Adv Polym Sci* 1967, 5, 59.
7. Staiti, P. *J New Mat Electrochem Systems* 2001, 4, 181.
8. Tazi, B.; Savadogo, O. *J New Mat Electrochem Systems* 2001, 4, 187.
9. (a) Rikukawa, M.; Sanui, K. *Prog Polym Sci* 2000, 25, 1463; (b) Hickner, M. A.; Ghassemi, H.; Kim, Y. S.; Einsla, B. R.; McGrath, J. E. *Chem Rev* 2004, 104, 4587; (c) Hamaya, T.; Inoue, S.; Qiao, J.; Okada, T. *J Power Sources* 2006 (Epub ahead of print).
10. Cheng, K. L.; Ueto, I. T. *Handbook of Organic Analytical Reagents*; CRC Press: Boca Raton, Florida, 1982; p 159.
11. Hirsch, R. F.; Gancher, E.; Russo, F. R. *Talanta* 1970, 17, 483.
12. Fritz, J. S.; Moyers, E. M. *Talanta* 1976, 23, 590.
13. Sun, S. F. *Physical Chemistry of Macromolecules: Basic Principles and Issues*; Wiley: New York, 1999.
14. Herrera, A. M.; García-Serrano, J.; Alvarado-Rodríguez, J. G.; Rivas-Silva, J. F.; Pal, U. *Acta Crystallogr Sect E* 2005, 61, m2752.
15. McQuade, D. T.; McKay, S. I.; Powell, D. R.; Gellman, S. H. *J Am Chem Soc* 1997, 119, 8528.
16. Silaghi-Dumitrescu, L.; Gibbons, M. N.; Silaghi-Dumitrescu, I.; Zukerman-Schpector, J.; Haiduc, I.; Sowerby, D. B. *J Organomet Chem* 1996, 517, 101.
17. (a) Gellman, S. H.; Dado, G. P.; Liang, G. B.; Adams, B. R. *J Am Chem Soc* 1991, 113, 1164; (b) Dado, G. P.; Gellman, S. H. *J Am Chem Soc* 1993, 115, 4228.